

Implications of the recent high statistics determination of the pion electromagnetic form factor in the timelike region

B. Ananthanarayan,¹ Irinel Caprini,² and I. Sentitemsu Imsong¹

¹*Centre for High Energy Physics, Indian Institute of Science, Bangalore 560 012, India*

²*National Institute of Physics and Nuclear Engineering
POB MG 6, Bucharest, R-76900, Romania*

The recently evaluated two-pion contribution to the muon $g - 2$ and the phase of the pion electromagnetic form factor in the elastic region, known from $\pi\pi$ scattering by Fermi-Watson theorem, are exploited by analytic techniques for finding correlations between the coefficients of the Taylor expansion at $t = 0$ and the values of the form factor at several points in the spacelike region. We do not use specific parametrizations and the results are fully independent of the unknown phase in the inelastic region. Using for instance, from recent determinations, $\langle r_\pi^2 \rangle = (0.435 \pm 0.005) \text{ fm}^2$ and $F(-1.6 \text{ GeV}^2) = 0.243^{+0.022}_{-0.014}$, we obtain the allowed ranges $3.75 \text{ GeV}^{-4} \lesssim c \lesssim 3.98 \text{ GeV}^{-4}$ and $9.91 \text{ GeV}^{-6} \lesssim d \lesssim 10.46 \text{ GeV}^{-6}$ for the curvature and the next Taylor coefficient, with a strong correlation between them. We also predict a large region in the complex plane where the form factor cannot have zeros.

PACS numbers: 11.55.Fv, 13.40.Gp, 25.80.Dj

I. INTRODUCTION

The pion electromagnetic form factor $F(t)$, defined by the matrix element

$$\langle \pi^+(p') | J_\mu^{\text{elm}} | \pi^+(p) \rangle = (p + p')_\mu F(t) \quad (1)$$

where $q = p - p'$ and $t = q^2$, plays a central role in strong interaction dynamics. From the general principles of quantum field theory, it follows that $F(t)$ is normalized to $F(0) = 1$ and is a real analytic function in the t -plane cut along the real axis from the unitarity threshold $t_+ = 4M_\pi^2$ to infinity. At low energies its properties are described by chiral perturbation theory (ChPT), the low energy effective theory of the strong interactions [1, 2], calculations of the pion form factor being available in ChPT up to two loops [3]-[6]. Lattice gauge theory has recently become another useful tool for the calculation of the form factor at low energies [7]. On the other hand, perturbative QCD predicts the behavior at large momenta along the spacelike axis, where $Q^2 \equiv -t > 0$. The leading order (LO) asymptotic term is [8]-[12]

$$F(-Q^2) \sim \frac{16\pi F_\pi^2 \alpha_s(Q^2)}{Q^2}, \quad Q^2 \rightarrow \infty, \quad (2)$$

where F_π is the pion decay constant and $\alpha_s(Q^2) = 4\pi/[9\ln(Q^2/\Lambda^2)]$ is the running strong coupling to one loop. Next-to-leading-order corrections to (2) were calculated by various groups [13]-[16]. As discussed, for instance in [10, 17, 18], the transition to the perturbative QCD regime seems to occur quite slowly in this case.

The experimental information available on the pion form factor is very rich. This quantity was measured at spacelike values $Q^2 > 0$ with increasing precision

from electron-pion scattering and pion electroproduction from nucleons [19]-[23]. On the timelike cut, where the form factor is complex, the Fermi-Watson theorem implies that in the elastic region its phase is equal to the phase-shift of the P -wave of the $\pi\pi$ amplitude, calculated recently with precision using Roy equations and fixed- t dispersion relations [24-26]. The modulus has been measured from the cross section of $e^+e^- \rightarrow \pi^+\pi^-$ by several groups in the past [27]-[36], and more recently to high accuracy by the BABAR [37] and KLOE [38, 39] collaborations. These data have been used for an accurate evaluation of the two-pion contribution to the muon anomalous magnetic moment [40, 41].

The constraints imposed on the pion form factor by analyticity and unitarity have been exploited in many works (the list [42]-[67] covers only partly a very rich literature). Different analytic representations, either as standard dispersion relations [17], phase (Omnès-type) [18, 46, 50, 52, 53, 65] or modulus [52] representations, as well as expansions based on conformal mappings [18, 46, 51] or Padé-type approximants [64], have been constructed in order to correlate the low- and high-energy properties of the form factor. Of special interest is the issue of the zeros of the form factor, investigated by means of dispersive sum-rules [18, 43-45, 52] or by the more powerful techniques of analytic optimization theory [42, 47, 48]. In [61-63, 66] similar functional-analytic techniques were applied for deriving bounds on the expansion coefficients at $t = 0$, from an weighted integral of the modulus squared along the cut, known from unitarity and dispersion relations for a related QCD correlator.

In the present paper we address the same problem, *i.e.* to find constraints on the coefficients appearing in the

Taylor expansion

$$F(t) = 1 + \frac{1}{6}\langle r_\pi^2 \rangle t + ct^2 + dt^3 + \dots \quad (3)$$

from a well-defined input on the timelike axis, and also include information coming from high precision experiments that measure the form factor in the spacelike region. We also consider the problem of the zeros, and obtain a region in the complex t -plane where zeros are excluded. The main reason of revisiting the problem is the recent high statistics measurement of the modulus $|F(t)|$ on the unitarity cut by BABAR [37] and KLOE [38, 39] experiments. As we will show, this information leads to stringent constraints, of a remarkable level for a prediction independent of any specific parametrization.

We apply a technique discussed in [61, 68], which makes use of information on both the phase and modulus, and was shown recently [69, 70] to place stringent bounds on the $K\pi$ weak form factors. As first input we use the Fermi-Watson theorem, according to which one has, modulo π ,

$$\text{Arg}[F(t + i\epsilon)] = \delta_1^1(t), \quad t_+ < t < t_{\text{in}}, \quad (4)$$

where $\delta_1^1(t)$ is the phase-shift of the P -wave of $\pi\pi$ elastic scattering and t_{in} the first inelastic threshold. As discussed previously [18, 46], inelasticity in the case of the pion vector form factor is negligible below the opening of $\pi\omega$ channel, so we take $t_{\text{in}} = (M_\pi + M_\omega)^2$. Below this energy, the phase $\delta_1^1(t)$ is known with precision from Roy equations and fixed- t dispersion relations for $\pi\pi$ scattering [24–26].

We also include information on the modulus, generically expressed by an integral relation

$$\frac{1}{\pi} \int_{t_{\text{in}}}^{\infty} dt \rho(t) |F(t)|^2 \leq I, \quad (5)$$

where $\rho(t)$ is a positive definite weight in the region of integration and I is a known quantity. Actually, (5) does not fully account for the present information on $|F(t)|$: indeed, except for a small region near the threshold $t_+ = 4M_\pi^2$, the modulus is measured also below the inelastic threshold t_{in} , i.e. $|F(t)|$ is measured more or less point-wise, at every t , not only in averaged form as in (5). In principle, the accurate knowledge of the phase and modulus on a region on the unitarity cut is sufficient to pin down the form factor everywhere due to analyticity. In practice, however, due to the well-known “instability” of analytic continuation, the uncertainties, however small, lead to solutions which are very different at points outside the original data interval. Therefore, we do not proceed by constructing parametrizations of the form factor on the timelike axis, but consider instead the global class of functions compatible with the adopted input, and derive constraints on various quantities of interest from this class of functions. As we shall see, even the input (5) leads to quite strong constraints on the properties of the form factor near $t = 0$ and in the complex plane. Thus

the chosen method is fully justified by the results that have been obtained.

A further open point is the choice of the weight $\rho(t)$ in (5). In principle, a large class of positive weights, leading to a convergent integral for $|F(t)|$ compatible with the asymptotic behavior (2), can be adopted. The optimal procedure is to vary $\rho(t)$ over a suitable admissible class and take the best result. This approach will be investigated in a future work. In the present paper we make the particular choice that corresponds to the two-pion contribution to the muon $g - 2$, when the weight $\rho(t)$ has the form

$$\rho(t) = \frac{\alpha^2 M_\mu^2 (t - t_+)^{3/2}}{12\pi t^{7/2}} K(t), \quad K(t) = \int_0^1 du \frac{(1-u)u^2}{1-u + M_\mu^2 u^2/t}, \quad (6)$$

and the right-hand side (rhs) of (5) is the two-pion contribution to the muon anomaly in the range $t > t_{\text{in}}$,

$$I = \hat{a}_\mu^{\pi\pi}. \quad (7)$$

The practical motivation of this particular choice is that an accurate evaluation of the two-pion contribution to the muon anomaly, taking into account the correlations between different points, is available from the refs. [40, 41]. As a result, this choice guarantees a very precise input. We must emphasize that, once the input (4)-(7) is adopted, the treatment is optimal and no information is lost. A posteriori, it turns out that the results given by this choice are quite stringent.

In addition to the above input from the timelike axis, we include the values of $F(t)$ measured experimentally at some spacelike points

$$F(t_n) = f_n \pm \delta f_n, \quad t_n < 0, \quad n = 1, \dots, N, \quad (8)$$

where we use the most recent high precision experimental information from [22, 23]. Thus, we will be employing as input Eqs. (4)-(8) in order to obtain correlations between the coefficients of the Taylor expansion (3). We will investigate also the issue of the possible zeros of the form factor, deriving regions where zeros are forbidden.

In Sec. II we briefly review the mathematical method and in Sec. III the experimental information that goes into our computation. In Sec. IV, we present our results for the parameters (c, d) and compare them with results available in the literature. In Sec. V we derive regions where zeros are excluded along the real axis and in the complex t -plane, and in Sec. VI some discussions and our conclusions are presented.

II. BASIC FORMULAE

For solving the problem we follow a mathematical method presented in [61, 68]. We first define the Omnès

function

$$\mathcal{O}(t) = \exp \left(\frac{t}{\pi} \int_{t_{\text{in}}}^{\infty} dt' \frac{\delta(t')}{t'(t' - t)} \right), \quad (9)$$

where $\delta(t) = \delta_1^1(t)$ for $t \leq t_{\text{in}}$, and is an arbitrary function, sufficiently smooth (*i.e.* Lipschitz continuous) for $t > t_{\text{in}}$. As shown in [68], the results do not depend on the choice of the function $\delta(t)$ for $t > t_{\text{in}}$. A crucial remark is that the function $h(t)$ defined by

$$F(t) = \mathcal{O}(t)h(t) \quad (10)$$

is analytic in the t -plane cut only for $t > t_{\text{in}}$. The equality (5), written in terms of $h(t)$ as

$$\frac{1}{\pi} \int_{t_{\text{in}}}^{\infty} dt \rho(t) |\mathcal{O}(t)|^2 |h(t)|^2 = \hat{a}_{\mu}^{\pi\pi}, \quad (11)$$

can be expressed in a canonical form, if we perform the conformal transformation

$$\tilde{z}(t) = \frac{\sqrt{t_{\text{in}}} - \sqrt{t_{\text{in}} - t}}{\sqrt{t_{\text{in}}} + \sqrt{t_{\text{in}} - t}}, \quad (12)$$

which maps the complex t -plane cut for $t > t_{\text{in}}$ onto the unit disk $|z| < 1$ in the z -plane defined by $z \equiv \tilde{z}(t)$, and define a function $g(z)$ analytic in $|z| < 1$ by

$$g(z) = w(z)\omega(z)F(\tilde{t}(z))[\mathcal{O}(\tilde{t}(z))]^{-1}. \quad (13)$$

In this relation $\tilde{t}(z)$ is the inverse of $z = \tilde{z}(t)$, for $\tilde{z}(t)$ as defined in (12), and the last two factors give the function $h(\tilde{t}(z))$ defined in (10), which is analytic in $|z| < 1$. Finally, $w(z)$ and $\omega(z)$ are outer functions, *i.e.* functions analytic and without zeros in $|z| < 1$, defined in terms of their modulus on the boundary, related to $\sqrt{\rho(t)}$ and $|\mathcal{O}(t)|$, respectively. Equivalent integral representations of the outer functions in terms of their modulus can be written either in the z or t variables. In particular, we use

$$w(z) = \exp \left[\frac{1}{2\pi} \int_0^{2\pi} d\theta \frac{\zeta + z}{\zeta - z} \ln |w(\zeta)| \right], \quad \zeta = \exp(i\theta), \quad (14)$$

where

$$|w(\zeta)|^2 = \rho(\tilde{t}(\zeta)) \left| \frac{d\tilde{t}(\zeta)}{d\zeta} \right|, \quad (15)$$

and

$$\omega(z) = \exp \left(\frac{\sqrt{t_{\text{in}} - \tilde{t}(z)}}{\pi} \int_{t_{\text{in}}}^{\infty} \frac{\ln |\mathcal{O}(t')| dt'}{\sqrt{t' - t_{\text{in}}(t' - \tilde{t}(z))}} \right). \quad (16)$$

Then (11) can be written as

$$\frac{1}{2\pi} \int_0^{2\pi} d\theta |g(\zeta)|^2 = \hat{a}_{\mu}^{\pi\pi}. \quad (17)$$

From (12) it follows that the origin $t = 0$ of the t -plane is mapped onto the origin $z = 0$ of the z -plane. Therefore, from (13) it follows that each coefficient $g_k \in R$ of the expansion

$$g(z) = g_0 + g_1 z + g_2 z^2 + g_3 z^3 + \dots \quad (18)$$

is expressed in terms of the coefficients of order lower or equal to k , of the Taylor expansion (3). Moreover, the values $F(t_n)$ of the form factor at a set of real points $t_n < 0$, $n = 1, 2, \dots, N$, lead to the values

$$g(z_n) = w(z_n)\omega(z_n)F(t_n)[\mathcal{O}(t_n)]^{-1}, \quad z_n = \tilde{z}(t_n). \quad (19)$$

Then the L^2 norm condition (17) implies the determinantal inequality (for a proof and older references see [68]):

$$\begin{vmatrix} \bar{I} & \bar{\xi}_1 & \bar{\xi}_2 & \dots & \bar{\xi}_N \\ \bar{\xi}_1 & \frac{\bar{\xi}_1^{2K}}{1 - z_1^2} & \frac{(z_1 z_2)^K}{1 - z_1 z_2} & \dots & \frac{(z_1 z_N)^K}{1 - z_1 z_N} \\ \bar{\xi}_2 & \frac{(z_1 z_2)^K}{1 - z_1 z_2} & \frac{(z_2)^{2K}}{1 - z_2^2} & \dots & \frac{(z_2 z_N)^K}{1 - z_2 z_N} \\ \vdots & \vdots & \vdots & \ddots & \vdots \\ \bar{\xi}_N & \frac{(z_1 z_N)^K}{1 - z_1 z_N} & \frac{(z_2 z_N)^K}{1 - z_2 z_N} & \dots & \frac{z_N^{2K}}{1 - z_N^2} \end{vmatrix} \geq 0, \quad (20)$$

where $K \geq 1$ is an arbitrary integer and

$$\bar{I} = \hat{a}_{\mu}^{\pi\pi} - \sum_{k=0}^{K-1} g_k^2, \quad \bar{\xi}_n = g(z_n) - \sum_{k=0}^{K-1} g_k z_n^k. \quad (21)$$

The same relation (20) holds if we replace $\hat{a}_{\mu}^{\pi\pi}$ by an upper bound of this quantity and the equality sign in (17) by the \leq sign. Moreover, as shown in [68], the results depend in a monotonic way on the value of the rhs of (17), becoming weaker when this value is increased.

The extension to the case of complex points t_n , which enters in pairs since $F(t^*) = F^*(t)$, is straightforward and will be discussed in Sec. V.

III. EXPERIMENTAL INPUT

We take $\sqrt{t_{\text{in}}} = 0.917$ GeV, which corresponds to the first important inelastic threshold, due to the $\omega\pi$ pair. The choice of a lower value of t_{in} is legitimate in the present formalism, and we will work also with $\sqrt{t_{\text{in}}} = 0.8$ GeV, which will allow us to compare the constraining power of the input conditions (4) and (5).

Very precise parametrizations of the phase-shift δ_1^1 are given in [24, 26]. We use as phenomenological input the phase parametrized as [26]

$$\cot \delta_1^1(t) = \frac{\sqrt{t}}{2k_{\pi}^3} (M_{\rho}^2 - t) \left(\frac{2M_{\pi}^3}{M_{\rho}^2 \sqrt{t}} + B_0 + B_1 \frac{\sqrt{t} - \sqrt{t_0 - t}}{\sqrt{t} + \sqrt{t_0 - t}} \right), \quad (22)$$

TABLE I: $\pi^+\pi^-$ contribution to the muon anomaly for energies above $\sqrt{t_{\text{in}}}$.

$\sqrt{t_{\text{in}}}$	$\hat{a}_{\mu}^{\pi\pi}$
0.800 GeV	95.23×10^{-10}
0.917 GeV	22.17×10^{-10}

where $k_{\pi} = \sqrt{t/4 - M_{\pi}^2}$ and

$$\begin{aligned} \sqrt{t_0} &= 1.05 \text{ GeV}, & M_{\rho} &= 773.6 \pm 0.9 \text{ MeV}, \\ B_0 &= 1.055 \pm 0.011, & B_1 &= 0.15 \pm 0.05. \end{aligned} \quad (23)$$

The function δ_1^1 obtained from (22) is practically identical with the phase-shift obtained in [24] from Roy equations for $\sqrt{t} \leq 0.8$ GeV. The uncertainty is very small and we have checked that the results are practically insensitive to the variation of the phase-shift within the errors.

Above t_{in} we use in (9) a smooth phase $\delta(t)$, which approaches asymptotically π . As shown in [68], the dependence on $\delta(t)$ of the functions \mathcal{O} and ω , defined in (9) and (16) respectively, exactly compensate each other, leading to results fully independent of the unknown phase in the inelastic region.

The two-pion contribution to muon anomaly was evaluated to great precision in [40, 41]. The most recent evaluation [41], based on all the available experimental data, gives for the total $\pi^+\pi^-$ contribution to muon anomaly the value $a_{\mu}^{\pi\pi} = (507.80 \pm 1.22 \pm 2.50 \pm 0.56) \times 10^{-10}$. In our method we need the specific contribution $\hat{a}_{\mu}^{\pi\pi}$ of the energies from $\sqrt{t_{\text{in}}}$ to infinity. The values given below¹ are based on the BABAR data [37], whose spectrum extends up to 3 GeV.

For the interval 0.917 - 3 GeV the two-pion contribution is $(21.73 \pm 0.24) \times 10^{-10}$. Increasing the central value by the error, and adding an estimate of about 0.2×10^{-10} for the interval from 3 GeV to ∞ , gives the close upper bound $\hat{a}_{\mu}^{\pi\pi} \leq 22.17 \times 10^{-10}$ for the two-pion contribution from 0.917 GeV to ∞ . As mentioned above, if we use in (17), instead of the exact value of $\hat{a}_{\mu}^{\pi\pi}$ an upper bound on this quantity, the results are still valid, but are weaker. In order to obtain results which are in the same time unbiased and stringent, we need a conservative and accurate estimate of $\hat{a}_{\mu}^{\pi\pi}$.

For the interval 0.8 - 3 GeV the two-pion contribution in [41] is $(94.25 \pm 0.77) \times 10^{-10}$. Increasing as before the central value by the error, and adding 0.2×10^{-10} for the interval from 3 GeV to ∞ , we obtain $\hat{a}_{\mu}^{\pi\pi} \leq 95.23 \times 10^{-10}$ for the two-pion contribution from 0.8 GeV to ∞ . The final numbers for the two choices of t_{in} are compiled in Table I.

¹ We are grateful to Bogdan Malaescu for providing us these numbers.

TABLE II: Spacelike data from [22, 23].

t	Value[GeV ²]	$F(t)$
t_1	-1.60	$0.243 \pm 0.012_{-0.008}^{+0.019}$
t_2	-2.45	$0.167 \pm 0.010_{-0.007}^{+0.013}$

Finally, we use additional spacelike data coming from [22, 23], which are collected for completeness in Table II, where the first error is statistical and the second is systematical.

IV. ALLOWED DOMAIN IN THE $c-d$ PLANE

In this section, we present the constraints on the coefficients c and d entering the Taylor expansion (3) using the formalism developed in Sec. II. We list in Table III the various quantities required in the basic inequality (20), for two choices of t_{in} . We implemented the normalization $F(0) = 1$, but kept arbitrary the charge radius $\langle r_{\pi}^2 \rangle$ and the spacelike values F_1 and F_2 . Using the input from Tables I and III, one obtains easily from (20) a convex quadratic condition for the coefficients c and d , represented as the interior of an ellipse in the $c-d$ plane.

We consider first the constraints obtained without any information at spacelike points, when the determinant (20) has only one element, \bar{I} , and the condition (20) becomes

$$g_0^2 + g_1^2 + g_2^2 + g_3^2 + \dots \leq \hat{a}_{\mu}^{\pi\pi}. \quad (24)$$

The quantities g_i are calculated for $t_{\text{in}} = (0.8 \text{ GeV})^2$ using the first line of Table I and the first column of Table III, and for $t_{\text{in}} = (0.917 \text{ GeV})^2$ using the quantities written in the second line of Table I and the second column of Table III.

In order to investigate the influence of the choice of the threshold t_{in} , we show in Fig.1 the domains obtained with the two values of t_{in} considered in Tables I and III. For convenience, we take $\langle r_{\pi}^2 \rangle = 0.43 \text{ fm}^2$ [25, 53–55]. The figure shows that the ellipse corresponding to $t_{\text{in}} = (0.917 \text{ GeV})^2$ is smaller and lies fully inside that of the ellipse with $t_{\text{in}} = (0.8 \text{ GeV})^2$, proving that the best results are obtained by exploiting the known phase along the whole elasticity region. Therefore, in what follows we shall adopt the choice $t_{\text{in}} = (0.917 \text{ GeV})^2$.

A precise estimate $\langle r_{\pi}^2 \rangle = (0.435 \pm 0.005) \text{ fm}^2$ is given in [25]. In Fig.2 we present the domains described by (20) for $t_{\text{in}} = (0.917 \text{ GeV})^2$ and two values of the charge radius $\langle r_{\pi}^2 \rangle = 0.43 \text{ fm}^2$ and $\langle r_{\pi}^2 \rangle = 0.44 \text{ fm}^2$ resulting from this estimate. The allowed domain is quite sensitive to the variation of $\langle r_{\pi}^2 \rangle$, being shifted towards the upper right end if $\langle r_{\pi}^2 \rangle$ is increased. To account for the uncertainty of the charge radius, we take as allowed domain

TABLE III: Tabulation of the quantities entering as input in (20) for obtaining the constraints on the c, d coefficients, for two choices of t_{in} . The numbers $z_n \equiv \tilde{z}(t_n)$ are obtained using (12) and t_n given in Table II. The numerical coefficients include the information on the phase below t_{in} and the normalization $F(0) = 1$, while the charge radius $\langle r_\pi^2 \rangle$ (expressed in fm^2) and the values $F_n \equiv F(t_n)$ are left arbitrary.

Quantity	$t_{\text{in}} = (0.8 \text{ GeV})^2$	$t_{\text{in}} = (0.917 \text{ GeV})^2$
g_0	0.2284×10^{-4}	0.1238×10^{-4}
g_1	$(0.2503\langle r_\pi^2 \rangle - 0.0414) \times 10^{-3}$	$(0.1783\langle r_\pi^2 \rangle - 0.0431) \times 10^{-3}$
g_2	$(0.1497c - 0.9547\langle r_\pi^2 \rangle - 0.1160) \times 10^{-3}$	$(0.1401c - 0.9773\langle r_\pi^2 \rangle - 0.0985) \times 10^{-3}$
g_3	$(-0.8704c + 0.3833d + 0.3879\langle r_\pi^2 \rangle - 0.7260) \times 10^{-3}$	$(-1.0481c + 0.4712d + 0.3589\langle r_\pi^2 \rangle - 0.9154) \times 10^{-3}$
z_1	-0.3033	-0.2603
z_2	-0.3745	-0.3285
$g(z_1)$	$F_1 \times 0.3051 \times 10^{-4}$	$F_1 \times 0.2066 \times 10^{-4}$
$g(z_2)$	$F_2 \times 0.3984 \times 10^{-4}$	$F_2 \times 0.2210 \times 10^{-4}$

the union of the two ellipses in Fig.2, which leads to the ranges

$$\begin{aligned} 3.48 \text{ GeV}^{-4} &\lesssim c \lesssim 3.98 \text{ GeV}^{-4}, \\ 9.36 \text{ GeV}^{-6} &\lesssim d \lesssim 10.46 \text{ GeV}^{-6}, \end{aligned} \quad (25)$$

with a strong correlation between the values of c and d .

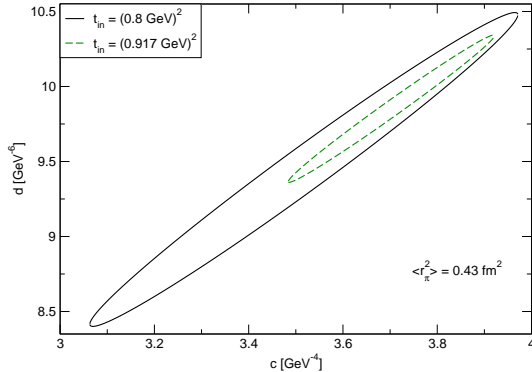


FIG. 1: Comparison of the $c - d$ domain obtained with $t_{\text{in}} = (0.917 \text{ GeV})^2$ and $t_{\text{in}} = (0.8 \text{ GeV})^2$ for $\langle r_\pi^2 \rangle = 0.43 \text{ fm}^2$.

We implement now the value at a point on the spacelike axis, using the input given in Table II. In this case the determinant in (20) has two rows and two columns. We choose the input at the spacelike point t_1 given in Table II and account for the errors by varying F_1 inside the error bars. In Fig. 3 we present the allowed domain in the $c - d$ plane obtained for $\langle r_\pi^2 \rangle = 0.43 \text{ fm}^2$ and three values of F_1 : the central value 0.243 given in Table II, and the extreme values 0.265 (0.228) obtained by adding (subtracting) the corresponding errors added in quadrature. The additional information on the spacelike axis improves in a dramatic way the constraints on the c and d coefficients. The small ellipses are entirely included in the larger ellipse obtained without information

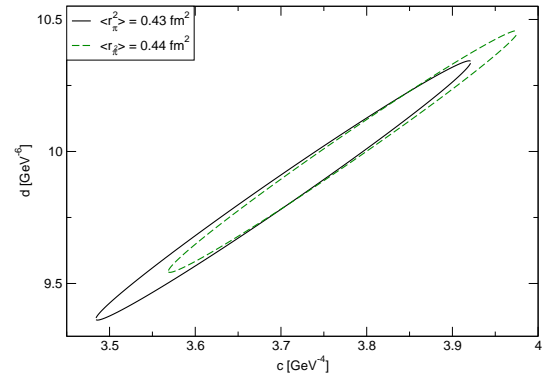


FIG. 2: Allowed domain in the $c - d$ plane obtained with $t_{\text{in}} = (0.917 \text{ GeV})^2$, for $\langle r_\pi^2 \rangle = 0.43 \text{ fm}^2$ and $\langle r_\pi^2 \rangle = 0.44 \text{ fm}^2$.

on the spacelike axis, which confirms the consistency of the various pieces of the input information. Varying F_1 inside the error bars, we obtain the allowed domain of the c and d parameters at the present level of knowledge as the union of the three small ellipses in Fig. 3. This gives, for $\langle r_\pi^2 \rangle = (0.435 \pm 0.005) \text{ fm}^2$, the allowed ranges

$$\begin{aligned} 3.75 \text{ GeV}^{-4} &\lesssim c \lesssim 3.98 \text{ GeV}^{-4}, \\ 9.91 \text{ GeV}^{-6} &\lesssim d \lesssim 10.45 \text{ GeV}^{-6}, \end{aligned} \quad (26)$$

with a strong correlation between the two coefficients. The comparison with (25) shows that the information at the spacelike point improves the lower bounds on both c and d , a feature seen actually from Fig. 3.

Similar results are obtained using as input the second Huber datum t_2 in Table II. Note that the formalism allows the simultaneous inclusion of several spacelike points in the determinant (20). In practice, as discussed in [62, 63], when more points are included the results are extremely sensitive to the values used as input, which requires adequate numerical methods for treating the problem.

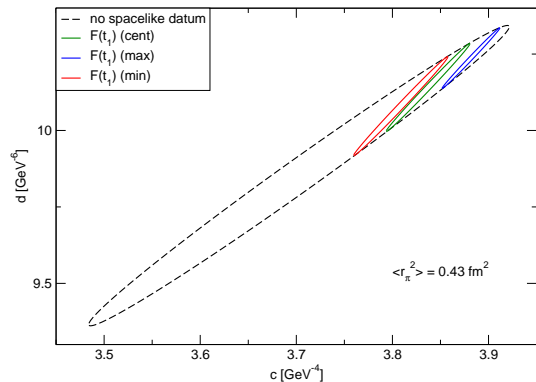


FIG. 3: Allowed domain in the $c - d$ plane calculated with $t_{in} = (0.917 \text{ GeV})^2$ and $\langle r_\pi^2 \rangle = 0.43 \text{ fm}^2$, for three values of $F(t_1)$ at the spacelike point $t_1 = -1.6 \text{ GeV}^2$ (central value in Table II and the extreme values obtained from the error intervals). Also shown is the large ellipse when no spacelike datum is included.

To illustrate the issues that arise in this context, a small digression is in order: the formalism presented in this work can be used to obtain limits on the value $F(t_2)$ at the second spacelike point, given the value $F(t_1)$ at the first one. This range results from the general inequality (20), written as

$$\begin{vmatrix} \hat{a}_\mu^{\pi\pi} - g_0^2 - g_1^2 & \bar{\xi}_1 & \bar{\xi}_2 \\ \bar{\xi}_1 & \frac{z_1^4}{1 - z_1^2} & \frac{(z_1 z_2)^2}{1 - z_1 z_2} \\ \bar{\xi}_2 & \frac{(z_1 z_2)^2}{1 - z_1 z_2} & \frac{(z_2)^4}{1 - z_2^2} \end{vmatrix} \geq 0, \quad (27)$$

where $z_i = \tilde{z}(t_i)$ and $\bar{\xi}_i = g(z_1) - g_0 - g_1 z_i$.

Using as input the coefficients given in the second column of Table III, we obtain from the above inequality a strong correlation between the values $F(t_1)$ and $F(t_2)$. For instance, taking the radius to be 0.435 fm^2 and $F(t_1)$ at its central value in Table II, (27) restricts $F(t_2)$ to the narrow range $(0.159, 0.173)$. The central experimental value of $F(t_2)$ quoted in Table II is contained in this range, which means that the central Huber values are consistent with each other in the analytic framework that we have adopted. On the other hand, taking $F(t_1)$ at the lower end of the experimental interval, we obtain the allowed range of $F(t_2)$ as $(0.135, 0.153)$, below the experimental interval, while fixing $F(t_1)$ at the upper end yields the range $(0.199, 0.201)$, above the experimental interval. It follows that an allowed range of $F(t_2)$ consistent with the experiment can be obtained only by reducing the input range of $F(t_1)$. By varying simultaneously the value of $F(t_1)$ and the radius, $\langle r_\pi^2 \rangle = (0.435 \pm 0.005) \text{ fm}^2$, we obtain for $F(t_2)$ the range $(0.130, 0.201)$, which may be expressed as $F(t_2) = 0.166 \pm 0.036$. The result is consistent with the numbers in Table II, but the error is a bit larger than the actual experimental one.

The digression above shows also that, by imposing simultaneously the experimental values at t_1 and t_2 , we can only obtain a slight improvement of the allowed domain of the parameters c and d . The reason is the fact that, as already noted above, the information on $F(t_2)$ forces $F(t_1)$ to lie within a slightly smaller range around the central value. Since the gain is expected to be small, we keep for simplicity as input only one spacelike point, which is sufficient to produce the narrow ranges reported in (26).

It is of interest to compare our predictions with previous determinations available in the literature. First, the range of c given in (26) considerably improves the bounds obtained with similar techniques in [61–63, 66]. The improvement is due mainly to the very accurate information available now on the modulus, expressed in the values in Table I. On the theoretical side, a fit based on ChPT to two-loop accuracy for τ decays gives $c = (3.2 \pm 0.5_{exp} \pm 0.9_{theor}) \text{ GeV}^{-4}$ [4]. Subsequent calculations of the electromagnetic form factors in two-loop ChPT lead to the values $c = (3.85 \pm 0.60) \text{ GeV}^{-4}$ [5], in agreement with the range given in (26), and $c = (4.49 \pm 0.28) \text{ GeV}^{-4}$ [6], slightly above that range. Finally, both the prediction $c = (4.00 \pm 0.50) \text{ GeV}^{-4}$, based on the quark-mass dependence of the form factor [65], and the range $c = (4 \pm 2) \text{ GeV}^{-4}$ quoted as a conservative next-to-next-to-leading ChPT result in the same reference, are consistent with (26). On the other hand, a recent lattice calculation with chiral extrapolation based on two-loop ChPT gives a slightly lower value, $c = 3.22(17)(36) \text{ GeV}^{-4}$ [7]. It must be noted however, that the lattice data are generated at rather high spacelike momenta, $t \in (-0.3, -1.7) \text{ GeV}^2$. Therefore the extraction of the radius and the curvature can not be very precise and the corresponding uncertainties might be larger than estimated.

Other determinations of the curvature are based on fits of experimental data with specific analytic parametrizations of the form factor. The value $c = (3.90 \pm 0.10) \text{ GeV}^{-4}$ was obtained in [59] by a usual dispersion relation, while a fit of the ALEPH data [57] on the hadronic τ decay rate with a Gounaris-Sakurai formula for the form factor [58] gives $c = (3.2 \pm 1.0) \text{ GeV}^{-4}$. Several analyses are based on phase (Omnès-type) representations, with various parametrizations of the phase along the whole unitarity cut. Their predictions, like $c = (3.79 \pm 0.04) \text{ GeV}^{-4}$ [53], $c = (3.84 \pm 0.02) \text{ GeV}^{-4}$ [55] and more recently $c = (3.75 \pm 0.33) \text{ GeV}^{-4}$ [65], are in overall agreement with (26). We note also that the value $c = (3.30 \pm 0.03_{stat} \pm 0.33_{syst}) \text{ GeV}^{-4}$, obtained recently from a fit of spacelike data with Padé approximants [64], is below our prediction (26). It may be worth investigating whether the fact that the unitarity cut and the precise data available along it are not included in this analysis is responsible for the mismatch.

As in the case of c , the range of d given in (26) considerably improves the bounds obtained with similar techniques in [61–63, 66]. The information available in the

literature on the cubic term in the Taylor expansion (3) is not rich. Theoretical results from ChPT and lattice calculations are not yet available. From fits of the data, the value $d = (9.70 \pm 0.40) \text{ GeV}^{-6}$ was obtained by means of usual dispersion relations in [59], while the Taylor expansion of the Gounaris-Sakurai parametrization [57], mentioned above, leads to $d = 9.80 \text{ GeV}^{-6}$. Both values are consistent with the range (26).

V. DOMAIN WHERE ZEROS ARE EXCLUDED

As we discussed in the Introduction (see also [70]), the formalism developed in Sec. II allows one to find rigorously the domain where the form factor cannot have zeros. The method amounts to testing the consistency of the assumption that a zero is present with the other pieces of the input. Let us assume first that $F(t)$ vanishes at some real point t_0 . From (13) it follows that $g(z_0) = 0$, where $z_0 = \tilde{z}(t_0)$. We therefore include this value in the determinant (20) and test the validity of the inequality: if it is satisfied, a zero is possible, if it is violated, the zero is forbidden. In particular, if we use only the information on the normalization $F(0) = 1$ and the charge radius, with no input on the spacelike axis, we obtain from (20) and (21) the following condition

$$\begin{vmatrix} \hat{a}_\mu^{\pi\pi} - g_0^2 - g_1^2 & -g_0 - g_1 z_0 \\ -g_0 - g_1 z_0 & \frac{z_0^4}{1 - z_0^2} \end{vmatrix} < 0, \quad (28)$$

for the points z_0 such that the form factor cannot vanish at $t_0 = \tilde{t}(z_0)$. Here g_0 and g_1 are expressed cf. Table III in terms of the charge radius.

If we include in addition the value at a point $z_1 = \tilde{z}(t_1)$, the condition reads

$$\begin{vmatrix} \hat{a}_\mu^{\pi\pi} - g_0^2 - g_1^2 & -g_0 - g_1 z_0 & \bar{\xi}_1 \\ -g_0 - g_1 z_0 & \frac{z_0^4}{1 - z_0^2} & \frac{(z_0 z_1)^2}{1 - z_0 z_1} \\ \bar{\xi}_1 & \frac{(z_0 z_1)^2}{1 - z_0 z_1} & \frac{(z_1)^4}{1 - z_1^2} \end{vmatrix} < 0, \quad (29)$$

with $\bar{\xi}_1 = g(z_1) - g_0 - g_1 z_1$.

With the values given in Tables I and III for $t_{\text{in}} = (0.917 \text{ GeV})^2$ and $\langle r_\pi^2 \rangle = 0.43 \text{ fm}^2$, the inequality (28) implies that simple zeros are excluded from the interval $-1.93 \text{ GeV}^2 \leq t_0 \leq 0.83 \text{ GeV}^2$ of the real axis. If we impose the additional constraint at a spacelike point $t_1 = -1.6 \text{ GeV}^2$, the interval for the excluded zeros is much bigger. The left end of the range is actually quite sensitive to the input value $F_1 = F(t_1)$. Using the central value $F_1 = 0.243$ given in Table II, we find from (29) that the form factor cannot have simple zeros in the range $-5.56 \text{ GeV}^2 \leq t_0 \leq 0.84 \text{ GeV}^2$. By varying F_1 inside the error interval given in Table II (with

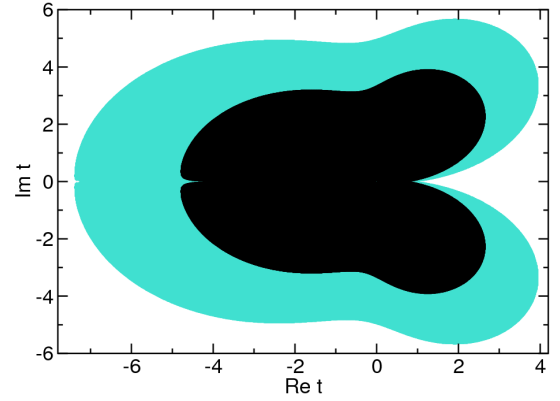


FIG. 4: Comparison of the domains without zeros obtained from (30) using $t_{\text{in}} = (0.8 \text{ GeV})^2$ (smaller domain) and $t_{\text{in}} = (0.917 \text{ GeV})^2$ (bigger domain), for $\langle r_\pi^2 \rangle = 0.43 \text{ fm}^2$.

errors added in quadrature), we find that zeros are excluded from the range $-12.67 \text{ GeV}^2 \leq t_0 \leq 0.84 \text{ GeV}^2$ for $F_1 = 0.265$ at the upper limit of the error interval, while for the lower limit $F_1 = 0.228$ the range is $-4.46 \text{ GeV}^2 \leq t_0 \leq 0.84 \text{ GeV}^2$.

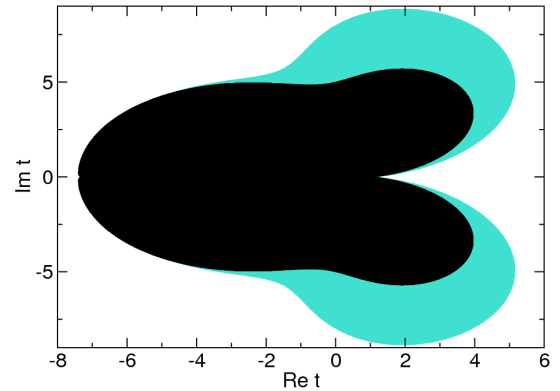


FIG. 5: Domain without zeros obtained from (30) using $t_{\text{in}} = (0.917 \text{ GeV})^2$, for two values of the pion charge radius, $\langle r_\pi^2 \rangle = 0.43 \text{ fm}^2$ (smaller domain) and $\langle r_\pi^2 \rangle = 0.44 \text{ fm}^2$ (bigger domain).

We now turn to the study of complex zeros. The formalism presented in Sec. II can be easily adapted to include complex values of the form factor outside the real axis. Since the form factor is real analytic, its zeros occur in complex conjugate pairs, *i.e.* if $F(t_0) = 0$, then also $F(t_0^*) = 0$ (a double zero occurs as t_0 approaches the real axis). One can show that the determinant condition (28)

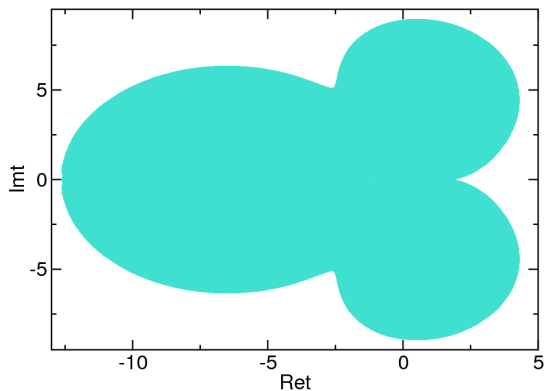


FIG. 6: Domain without zeros obtained with $t_{\text{in}} = (0.917 \text{ GeV})^2$ and $\langle r_\pi^2 \rangle = 0.43 \text{ fm}^2$, using in addition the central experimental value $F(t_1) = 0.243$ at the spacelike point $t_1 = -1.6 \text{ GeV}^2$.

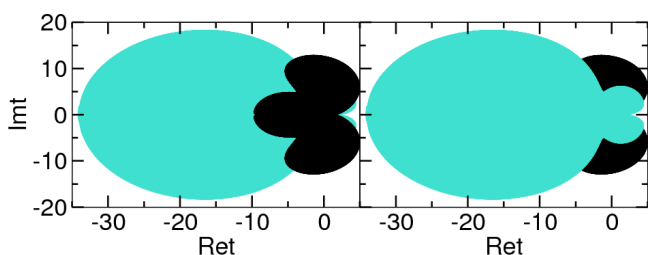


FIG. 7: Comparison of the domains with no zeros obtained with $t_{\text{in}} = (0.917 \text{ GeV})^2$ and $\langle r_\pi^2 \rangle = 0.43 \text{ fm}^2$, for the spacelike input $F_1 = 0.265$ (bigger domain) and $F_1 = 0.228$ (smaller domain).

for the domain without zeros is generalized to

$$\begin{vmatrix} \hat{a}_\mu^{\pi\pi} - g_0^2 - g_1^2 & -g_0 - g_1 z_0 & -g_0 - g_1 z_0^* \\ -g_0 - g_1 z_0^* & \frac{(z_0 z_0^*)^2}{1 - |z_0|^2} & \frac{(z_0^*)^4}{1 - (z_0^*)^2} \\ -g_0 - g_1 z_0 & \frac{z_0^4}{1 - z_0^2} & \frac{(z_0 z_0^*)^2}{1 - |z_0|^2} \end{vmatrix} < 0. \quad (30)$$

The determinant is real since the corresponding matrix is Hermitian. The 4×4 determinant that includes in addition a value at a spacelike point t_1 can be easily written down.

We first apply the inequality (30) to illustrate the dependence of the domain without zeros on the value of t_{in} used in the calculations. As seen from Fig.4, the larger value $t_{\text{in}} = (0.917 \text{ GeV})^2$ leads to a domain that extends to high values of $|t|$ in all the directions of the complex plane, which shows that, like in the case of the $c - d$ domain, the best results are obtained if the phase condition (4) is used along the whole range of validity.

The dependence of the domain on the variation of $\langle r_\pi^2 \rangle$ is shown in Fig.5. As expected, for a larger charge radius,

$\langle r_\pi^2 \rangle = 0.44 \text{ fm}^2$, the zeros are excluded from a bigger complex domain around the timelike axis, while the left end of the domain, around the spacelike axis, is almost insensitive to the slope at $t = 0$.

The effect of an additional input at a spacelike point is illustrated in Fig.6, where we show the domain in the complex plane where zeros are excluded, using $t_1 = -1.6 \text{ GeV}^2$ and the value $F(t_1) = 0.243$ (the central experimental value given in [22, 23]). By comparing Fig.6 with the large domain in Fig.4, one can see that the knowledge of the form factor at a spacelike point excludes zeros in a larger domain near the spacelike axis, while it has a smaller influence on the right part of the domain. This feature is present also in Fig.7, which shows the sensitivity of the domain to the input value of $F(t_1)$. As is seen in the figure, the larger value $F(t_1) = 0.265$ obtained from the upper limit of the error bar, excludes the zeros in a domain extending to considerably larger values along the spacelike axis.

The results on the zeros reported in the literature [18, 42–44, 47, 48] are rather controversial. The best results for the regions free of zeros were obtained in [42, 47, 48], by a method related to ours. However, since the experimental information at that time was poor, the authors were forced to make some ad-hoc assumptions, especially on the modulus on the timelike axis. At present the precise measurement of the modulus gives a solid basis to our results.

The issue of zeros is of relevance for the analytic representation of the form factor using phase (Omnès)- or modulus-type representations, which require the knowledge of the zeros. Such representations were extensively studied in the past [18, 46, 50, 52, 53, 65], and often are based on the assumption that zeros are absent. Our results, which show that the zeros are excluded from a rather large region at low energies, give support to such representations, and confirm also theoretical expectations based on ChPT or more general physical arguments [18].

VI. DISCUSSIONS AND CONCLUSION

The experimental information available at present on the pion electromagnetic form factor is very rich. The recent high statistics measurements of the modulus by BABAR and KLOE collaborations [37–39], supplemented by the phase in the elastic region known with accuracy from the P -wave of $\pi\pi$ scattering [24–26], are expected to considerably constrain the behavior on the timelike axis. The values of the form factor on the spacelike axis are also measured with increasing precision. Theoretically, predictions on the pion form factor at low energies are available from ChPT and lattice QCD, while perturbative QCD predicts the behavior at high energies along the spacelike axis. The transition to the perturbative regime is known to be an open problem that deserves further study in the case of the pion form factor.

Analyticity is the ideal tool for connecting the low- and high-energy regimes for physical quantities like the pion form factor. The full treatment of the present rich experimental and theoretical input, which might overconstrain the system, is a challenge for the future investigations based on analyticity. In the present work we do not perform such a complete analysis, but exploit only in part the present information on the modulus on the unitarity cut. However, even in this limited frame we obtain quite stringent conclusions on the low energy properties of the form factor.

The conditions used as input in our approach are expressed by the phase condition (4) and the integral of the modulus squared (5), which we further restricted by choosing the weight $\rho(t)$ as the kernel relevant for the two-pion contribution to the muon anomaly, cf. (6) and (7). A more general class of suitable weights will be investigated in a future work. Once the input is chosen, it is exploited in an optimal way by a mathematical formalism presented in Sec. II, leading to strong correlations between the coefficients of the Taylor expansion (3) at $t = 0$ and the values of the form factor on the spacelike axis.

Our basic results are contained in Eqs. (20) and (21), where the input quantities are defined in Tables I-III. The numerical coefficients in Table III depend on the normalization $F(0) = 1$ and the phase of the form factor below the inelastic threshold t_{in} , being very stable with respect to small variations of the phase. Moreover, as emphasized in Sec. II, the results are independent of the unknown phase of the form factor above the inelastic threshold t_{in} . In Table III, the charge radius $\langle r_\pi^2 \rangle$, the higher-order Taylor coefficients c and d , and the values of the form factor at several spacelike points are kept free, so the formalism can be easily applied for finding model independent correlations between the values of the form factor at different points and for testing the consistency of input values known from different sources.

In Sec. IV we derived stringent constraints on the allowed values of the higher-order coefficients c and d of the Taylor expansion (3). The best results are obtained with $t_{\text{in}} = (0.917 \text{ GeV})^2$, which corresponds to the physical inelastic threshold produced by the $\omega\pi$ channel. The charge radius and an additional information at a spacelike point were used as input. In (25) and (26) and in Figs. 1 - Fig. 3 we illustrated the results for $\langle r_\pi^2 \rangle$ in the range $(0.43 - 0.44) \text{ fm}^2$ and $F(-1.6 \text{ GeV}^2) = 0.243 \pm 0.012_{-0.008}^{+0.019}$ [22, 23]. It is remarkable that the allowed ranges are already comparable in precision with other determinations in the literature based on specific parametrizations.

The present method can be used also to obtain bounds on the values of the form factor along the spacelike axis, using as input the information on the timelike axis, together with some values inside the analyticity domain. As discussed in Sec. IV, using as input the value $F(t_1)$ at the first Huber point, we obtain stringent limits on the value $F(t_2)$ at the second point, with a strong correlation

between the two. Of course, the method can be applied in principle also to higher spacelike energies. However, with our choice of the weight ρ , we expect that the predictions will become gradually weaker when the energy is increased. Indeed, since ρ decreases rapidly at large momenta, the condition (5) provides stringent constraints on the low energy parameters like c and d , but in the same time it imposes weak constraints on the behavior of the form factor at large energies. A different choice of ρ could lead to interesting results also for the behavior at higher energies, but this is beyond the scope of the present analysis and will be investigated in a future work.

In Sec. V we showed that the same formalism leads to an analytic description for the regions of the complex plane where the zeros of the form factor are forbidden. Our results are contained in Eqs. (28)-(30) and are illustrated in Figs. (4) - (7), for the same input $\langle r_\pi^2 \rangle$ and $F(t_1)$. We obtain a rather large domain where zeros are excluded, which gives support to Omnès-type representations, which often assume the absence of the zeros. Our results also confirm theoretical expectations on the absence of zeros at low energy, based on ChPT or general physical arguments [18]. We note that by our method we can find rigorously the domains free of zeros, but we can say nothing about the remaining domains, where zeros may be present or absent. Alternative methods, based on modulus representations [18, 43, 52], can rule out in principle the zeros from the whole complex plane provided they are absent. However, these methods are very sensitive to the input and led to controversial results in the past. An update of such analyses using the recent precise determination of the modulus would be of much interest.

We finally note that the mathematical formalism applied in this paper may be useful also for finding an analytic parametrization of the form factor suitable for fitting the rich amount of experimental data. Namely, the representation of $F(t)$ that results from (13) involves the known functions $w(z)$, which accounts for the weight $\rho(t)$, $\omega(z)$ and $\mathcal{O}(t)$, which implement the phase below t_{in} , and the arbitrary function $g(z)$, analytic in the t -plane cut for $t > t_{\text{in}}$, or equivalently in the unit disc $|z| < 1$ of the z -plane defined by the conformal mapping (12). The expansion (18) is convergent in $|z| < 1$, and moreover the coefficients satisfy the inequality (24), which is very useful in order to control the higher orders of the expansion and the truncation error.

Acknowledgement: BA thanks the Department of Science and Technology, the Government of India, and the Homi Bhabha Fellowships Council for support. IC acknowledges support from CNCSIS in the Program Idei, Contract No. 464/2009. We thank B. Malaescu, G. Colangelo, M. Passera and S. Ramanan for useful correspondence.

-
- [1] S. Weinberg, *Physica A: Statistical and Theoretical Physics* **96**, 327 (1979).
- [2] J. Gasser and H. Leutwyler, *Nucl. Phys. B* **250**, 465 (1985).
- [3] J. Gasser and U.G. Meissner, *Nucl. Phys. B* **357**, 90 (1991).
- [4] G. Colangelo, M. Finkemeier and R. Urech, *Phys. Rev. D* **54**, 4403 (1996) [arXiv:hep-ph/9604279].
- [5] J. Bijnens, G. Colangelo and P. Talavera, *JHEP* **9805**, 014 (1998) [arXiv:hep-ph/9805389].
- [6] J. Bijnens and P. Talavera, *JHEP* **0203**, 046 (2002) [arXiv:hep-ph/0203049].
- [7] S. Aoki *et al.* [JLQCD Collaboration and TWQCD Collaboration], *Phys. Rev. D* **80**, 034508 (2009) [arXiv:0905.2465 [hep-lat]].
- [8] G. R. Farrar and D. R. Jackson, *Phys. Rev. Lett.* **43**, 246 (1979).
- [9] G. P. Lepage and S. J. Brodsky, *Phys. Rev. D* **22**, 2157 (1980).
- [10] A. V. Efremov and A. V. Radyushkin, *Phys. Lett. B* **94**, 245 (1980).
- [11] V. L. Chernyak and A. R. Zhitnitsky, *JETP Lett.* **25**, 510 (1977) [*Pisma Zh. Eksp. Teor. Fiz.* **25**, 544 (1977)].
- [12] V. L. Chernyak and A. R. Zhitnitsky, *Sov. J. Nucl. Phys.* **31**, 544 (1980) [*Yad. Fiz.* **31**, 1053 (1980)].
- [13] B. Melic, B. Nizic and K. Passek, *Phys. Rev. D* **60**, 074004 (1999) [arXiv:hep-ph/9802204].
- [14] V. M. Braun, A. Khodjamirian and M. Maul, *Phys. Rev. D* **61**, 073004 (2000) [arXiv:hep-ph/9907495].
- [15] J. Bijnens and A. Khodjamirian, *Eur. Phys. J. C* **26**, 67 (2002) [arXiv:hep-ph/0206252].
- [16] J. W. Chen, H. Kohyama, K. Ohnishi, U. Raha and Y. L. Shen, *Phys. Lett. B* **693**, 102 (2010) [arXiv:0908.2973 [hep-ph]].
- [17] J. F. Donoghue and E. S. Na, *Phys. Rev. D* **56**, 7073 (1997) [arXiv:hep-ph/9611418].
- [18] H. Leutwyler, arXiv:hep-ph/0212324.
- [19] C.J. Bebek *et al.*, *Phys. Rev. D* **17**, 1693 (1978).
- [20] S.R. Amendolia *et al.* [NA7 Collaboration], *Nucl. Phys. B* **277**, 168 (1986).
- [21] V. Tadevosyan *et al.* [Jefferson Lab F(π) Collaboration], *Phys. Rev. C* **75**, 055205 (2007) [arXiv:nucl-ex/0607007].
- [22] T. Horn *et al.* [Jefferson Lab F(π)-2 Collaboration], *Phys. Rev. Lett.* **97**, 192001 (2006) [arXiv:nucl-ex/0607005].
- [23] G.M. Huber *et al.* [Jefferson Lab Collaboration], *Phys. Rev. C* **78**, 045203 (2008) [arXiv:0809.3052 [nucl-ex]].
- [24] B. Ananthanarayan, G. Colangelo, J. Gasser and H. Leutwyler, *Phys. Rept.* **353**, 207 (2001) [arXiv:hep-ph/0005297].
- [25] G. Colangelo, J. Gasser and H. Leutwyler, *Nucl. Phys. B* **603**, 125 (2001) [arXiv:hep-ph/0103088].
- [26] R. Kaminski, J. R. Pelaez and F. J. Yndurain, *Phys. Rev. D* **77**, 054015 (2008) [arXiv:0710.1150 [hep-ph]].
- [27] L. M. Barkov *et al.*, *Nucl. Phys. B* **256**, 365 (1985).
- [28] I. B. Vasserman, *et al.*, *Sov. J. Nucl. Phys.* **30**, 519 (1979) [*Yad. Fiz.* **30**, 999 (1979)].
- [29] I. B. Vasserman *et al.*, *Yad. Fiz.* **33**, 709 (1981) [*Sov. J. Nucl. Phys.* **33**, 368 (1981)].
- [30] R. R. Akhmetshin *et al.* [CMD-2 Collaboration], *Phys. Lett. B* **578**, 285 (2004) [arXiv:hep-ex/0308008].
- [31] V. M. Aul'chenko *et al.* [CMD-2 Collaboration], *Pis'ma Zh. Eksp. Teor. Fiz.* **82**, 841 (2005) [*JETP Lett.* **82**, 743 (2005)] [arXiv:hep-ex/0603021].
- [32] V. M. Aul'chenko *et al.*, *Pis'ma Zh. Eksp. Teor. Fiz.* **84**, 491 (2006) [*JETP Lett.* **84**, 413 (2006)]. [arXiv:hep-ex/0610016].
- [33] R. R. Akhmetshin *et al.* [CMD-2 Collaboration], *Phys. Lett. B* **648**, 28 (2007) [arXiv:hep-ex/0610021].
- [34] M. N. Achasov *et al.*, *J. Exp. Theor. Phys.* **103**, 380 (2006) [*Zh. Eksp. Teor. Fiz.* **130**, 437 (2006)] [arXiv:hep-ex/0605013].
- [35] A. Quenzer *et al.*, *Phys. Lett. B* **76**, 512 (1978).
- [36] D. Bisello *et al.* [DM2 Collaboration], *Phys. Lett. B* **220**, 321 (1989).
- [37] B. Aubert *et al.* [BABAR Collaboration], *Phys. Rev. Lett.* **103**, 231801 (2009) [arXiv:0908.3589 [hep-ex]].
- [38] F. Ambrosino *et al.* [KLOE Collaboration], *Phys. Lett. B* **670**, 285 (2009) [arXiv:0809.3950 [hep-ex]].
- [39] F. Ambrosino *et al.* [KLOE Collaboration], arXiv:1006.5313 [hep-ex].
- [40] M. Davier, A. Hoecker, B. Malaescu, C. Z. Yuan and Z. Zhang, *Eur. Phys. J. C* **66**, 1 (2010) [arXiv:0908.4300 [hep-ph]].
- [41] M. Davier, A. Hoecker, B. Malaescu and Z. Zhang, *Eur. Phys. J. C* **71**, 1 (2011), arXiv:1010.4180 [hep-ph].
- [42] I. Raszillier, *Commun. Math. Phys.* **26**, 121 (1972).
- [43] C. Cronstrom, *Phys. Lett. B* **49**, 283 (1974).
- [44] S. Dubnicka and V.A. Meshcheryakov, *Nucl. Phys. B* **83**, 311 (1974).
- [45] Yu. P. Shcherbin, *Nucl. Phys. B* **112**, 470 (1976).
- [46] C. B. Lang and I. S. Stefanescu, *Phys. Lett. B* **58**, 450 (1975).
- [47] I. Raszillier, W. Schmidt and I. S. Stefanescu, *Z. Phys. A* **277**, 211 (1976).
- [48] I. Raszillier, W. Schmidt and I. S. Stefanescu, *J. Math. Phys. (N.Y.)* **17**, 1957 (1976).
- [49] M. F. Heyn and C. B. Lang, *Z. Phys. C* **7**, 169 (1981).
- [50] F. Guerrero and A. Pich, *Phys. Lett. B* **412**, 382 (1997) [arXiv:hep-ph/9707347].
- [51] W. W. Buck and R. F. Lebed, *Phys. Rev. D* **58**, 056001 (1998) [arXiv:hep-ph/9802369].
- [52] B.V. Geshkenbein, *Phys. Rev. D* **61**, 033009 (2000) [arXiv:hep-ph/9806418].
- [53] A. Pich and J. Portoles, *Phys. Rev. D* **63**, 093005 (2001) [arXiv:hep-ph/0101194].
- [54] J. F. De Troconiz and F. J. Yndurain, *Phys. Rev. D* **65**, 093001 (2002) [arXiv:hep-ph/0106025].
- [55] J. F. de Troconiz and F. J. Yndurain, *Phys. Rev. D* **71**, 073008 (2005) [arXiv:hep-ph/0402285].
- [56] G. Colangelo, *Nucl. Phys. B Proc. Suppl.* **131**, 185 (2004) [arXiv:hep-ph/0312017].
- [57] R. Barate *et al.* [ALEPH Collaboration], *Z. Phys. C* **76**, 15 (1997).
- [58] G. J. Gounaris and J. J. Sakurai, *Phys. Rev. Lett.* **21**, 244 (1968).
- [59] T. N. Truong, arXiv:hep-ph/9809476.
- [60] M. Davier, L. Girlanda, A. Hocker and J. Stern, *Phys. Rev. D* **58**, 096014 (1998) [arXiv:hep-ph/9802447].
- [61] I. Caprini, *Eur. Phys. J. C* **13**, 471 (2000) [arXiv:hep-ph/9907227].
- [62] B. Ananthanarayan and S. Ramanan, *Eur. Phys. J. C*

- 54**, 461 (2008) [arXiv:0801.2023 [hep-ph]].
- [63] B. Ananthanarayan and S. Ramanan, Eur. Phys. J. C **60**, 73 (2009) [arXiv:0811.0482 [hep-ph]].
 - [64] P. Masjuan, S. Peris and J. J. Sanz-Cillero, Phys. Rev. D **78**, 074028 (2008) [arXiv:0807.4893 [hep-ph]].
 - [65] F. K. Guo, C. Hanhart, F. J. Llanes-Estrada and U. G. Meissner, Phys. Lett. B **678**, 90 (2009) [arXiv:0812.3270 [hep-ph]].
 - [66] G. Abbas, B. Ananthanarayan and S. Ramanan, Eur. Phys. J. A **41**, 93 (2009), [arXiv:0903.4297 [hep-ph]].
 - [67] M. Belicka, S. Dubnicka, A. Z. Dubnickova and A. Liptaj, Phys. Rev. C **83**, 028201 (2011), [arXiv:1102.3122 [hep-ph]].
 - [68] G. Abbas, B. Ananthanarayan, I. Caprini, I.S. Imsong and S. Ramanan, Eur. Phys. J. A **45**, 389 (2010), [arXiv:1004.4257 [hep-ph]].
 - [69] G. Abbas, B. Ananthanarayan, I. Caprini, I. Sentitemsu Imsong and S. Ramanan, Eur. Phys. J. A **44**, 175 (2010) [arXiv:0912.2831 [hep-ph]].
 - [70] G. Abbas, B. Ananthanarayan, I. Caprini and I. Sentitemsu Imsong, Phys. Rev. D **82**, 094018 (2010) [arXiv:1008.0925 [hep-ph]].